Ultramafic inclusions in late Miocene alkaline basalts from Fry and Ruby Mountains, San Bernardino County, California

S. L. Neville, Peter Schiffman[1], and Peter Sadler

Department of Earth Sciences
University of California, Riverside, California 92521

Abstract

Flows, dikes, and remnant constructional features of ultramafic inclusion-bearing alkaline basalts, well known from the central Mojave, are also present near its southern boundary with the San Andreas fault at Fry and Ruby Mountains. Ultramafic inclusions from these localities are predominantly spinel lherzolites and harzburgites. A single, 200-gram garnet websterite inclusion found at Fry Mountain is only the second one reported in alkaline basalt from the western United States. All ultramafic inclusions from these localities exhibit tectonic textures and are believed to be accidental fragments of upper mantle material incorporated into basanite melts at temperatures between 950 and 1200°C and pressures between 9 and 23 kbar. Inclusion-bearing basaltic volcanism in the Fry and Ruby Mountain areas occurred between 6 and 10 million years ago, whereas comparable volcanism in the central Mojave beyond the transpressional tectonism of the San Andreas fault has continued into the Quaternary.

Introduction

Studies of ultramafic inclusions provide crucial input for models concerning the thermal structure of the upper mantle and the origin of alkaline basaltic melts. Compositional data on the coexisting minerals in these inclusions can be used to estimate the pressure and temperature conditions of their source regions. Ultramafic inclusions from the central Mojave Desert of California have been extensively studied (e.g., at Dish Hill by Wise, 1966 and 1969; Wilshire et al., 1971 and 1980; Wilshire and Trask, 1971; and at the Cima volcanic field by Katz and Boettcher, 1980). This paper presents petrologic data and thermobarometric calculations for a suite of ultramafic inclusions from two new localities near the southern margin of the Mojave Desert. These may represent the oldest occurrences of ultramafic inclusion-bearing alkaline basalts in the Mojave Desert. The Fry Mountain locality is of particular significance because a garnet websterite inclusion found there is only the second such described from alkaline basalts in the western United States.

Geologic setting

Fry Mountain (34°30′N, 116°43′W) and Ruby Mountain (34°16′N, 116°40′W) are the two most prolific ultramafic inclusion localities within an approximately 1000 square kilometer area of predominantly inclusion-free alkaline basaltic volcanism in the south central Mojave Desert and adjacent San Bernardino Mountains (Fig. 1). At these localities, ultramafic inclusions, ranging in size from 1 to 12

cm, occur within both flows and the exposed feeder dikes which have intruded Mesozoic plutonic rocks. Cinder cones, common in central Mojave ultramafic inclusion localities, are rare and where present (e.g., at Fry Mountain) are deeply dissected (see Neville, 1982 and Neville and Chambers, 1982 for detailed descriptions of field relations.)

Alkaline basalts in the Fry and Ruby Mountain areas are older than those of the central Mojave. Radiometric age determinations on alkaline basalts from the area shown in Figure 1 range from 6 to 9 m.y. (Peterson, 1976; Oberlander, 1972). One inclusion-bearing flow at Fry Mountain has been dated by K/Ar at 8.9 ± 0.2 m.y. The oldest flows in the central Mojave are very late Miocene (7.6 m.y. in the Cima Field according to Dohrenwend et al., 1984), although inclusion-bearing volcanism has been active until at least the late Pliocene: Katz and Boettcher (1980) report a carbon 14 date of 330–480 years on charcoal from a Cima flow.

Basalt and megacryst petrography and chemistry

The alkaline basalts from Fry and Ruby Mountains are markedly uniform in their petrographic characteristics. These rocks are fine-grained and sparsely phyric; microphenocrysts generally comprise less than 15% of the mode and include olivine (0.75 mm) and lesser titaniferous augite (0.50 mm). Pilotaxitic groundmass minerals include olivine, clinopyroxene, plagioclase, Fe-Ti oxides, apatite, and in some samples phlogopite. Deuteric zeolites (natrolite and analcite?) occur interstitially in the groundmass, in microfractures, and in vesicles. Megacrysts found in flows which contain ultramafic inclusions include: (1) strained anhedral olivine (up to 3.5 cm) at Fry Mountain; (2) translucent, white anorthoclase ($Ab_{78}Or_{17}An_{05}$) at Ruby Mountain;

Fig. 1. Ultramafic inclusion localities in the south-central Mojave Desert and adjacent San Bernardino Mountains. The inset map in the upper right shows the location of other major Mojave Desert alkaline basalt localities including: Amboy Crater (A), Cima Dome (C), Dish Hill (D), Malapi Hill (M), and Pisgah Crater (P). Generalized geologic units shown include: pre-Tertiary basement (stippled), late Tertiary ultramafic inclusion-absent alkaline basalts (diagonal rule), late Tertiary ultramafic inclusion-bearing alkaline basalts (solid black), and alluvium (white).

and black, vitreous, conchoidally fractured (3) clinopyroxene and (4) kaersutite (both up to 5 cm) at both Fry and Ruby Mountains. Kaersutites typically exhibit some traces of cleavage whereas clinopyroxene megacrysts do not.

Whole rock, major element analyses of basalts (minus inclusions if present) were determined by atomic absorption and X-ray fluorescence spectroscopy (see Neville, 1982 for analytical procedures). Representative analyses are presented in Table 1. According to the classification of Wise (1969), all of the basalts analyzed are basanites (i.e., with $SiO_2 < 46$ wt.%, normative nepheline > 5%, and K_2O > 1.5 wt.%.) The alkali variation diagram of Figure 2a demonstrates the limited SiO_2 compositional variation of the basalts from Ruby and Fry Mountains (closed circles) as well as other petrographically similar inclusion-bearing and inclusion-free basalts from localities depicted in Figure 1. As can be seen in Figure 2a, alkali basalts from younger, central Mojave Desert localities (open symbols) are generally more SiO_2-rich. A better discriminant for distinguishing these two suites of alkaline basalts is their TiO_2–MgO relationships (Fig. 2b). The basalts of the Fry and Ruby Mountain suite are generally enriched in TiO_2 and MgO with respect to the basalts of the Central Mojave suite.

Basalts of the Fry and Ruby Mountain suite are compo-

sitionally identical, excluding inclusions, whether they are inclusion-bearing or inclusion-free. However, basalts which contain relatively high modal abundances (approximately 5%) of kaersutite and clinopyroxene megacrysts are TiO_2-poorer than basalts with lesser megacryst contents.

Inclusion petrography

Thirteen ultramafic inclusions from Fry Mountain and 26 from Ruby Mountain were analyzed modally, with 400–500 points counted on each sample. Modal compositions of these samples, shown in Figure 3, indicate that lherzolite and subordinate harzburgite are the most common inclusion types. Additional identified ultramafic lithologies comprise singular occurrences of garnet websterite (Fry Mountain), olivine websterite (Ruby Mountain), and amphibole-olivine websterite (Fry Mountain). All of the spinel lherzolite and harzburgite inclusions have petrographic characteristics of the Cr-diopside series of Wilshire and Shervais (1975).

Spinel lherzolite inclusions (Fig. 4) are composed of a mosaic of anhedral forsteritic olivine (1.0 to 3.0 mm), anhedral to subhedral enstatite (1.0 to 3.5 mm, colorless with common clinopyroxene exsolution lamellae approximately 2 microns thick), anhedral diopside (0.5 to 1.0 mm and colorless, with rare orthopyroxene exsolution lamellae), and anhedral brown to green spinel (0.5 to 1.0 mm), which comprises up to 3% of the total mode. Texturally, spinel lherzolites are porphyroclastic (Pike and Schwarzman, 1977), and characterized by kinked or strained porphyroclasts set

Table 1. Composition of alkaline basalts from Fry and Ruby Mountain, California

|	Fry Mountain						Ruby Mt.	
	FMA-2	FMA-6	FMG-32	FMCS-31	FMCS-32	FMG-34	RM-3	RM-20
SiO_2	44.19	44.89	43.14	43.80	42.82	44.10	44.65	45.26
TiO_2	3.66	3.43	3.22	3.54	3.69	3.19	2.59	2.61
Al_2O_3	15.16	15.78	14.39	16.65	14.23	14.38	15.92	15.99
FeO	11.94	10.47	10.97	11.34	12.66	11.09	12.64	12.54
MnO	0.20	0.19	0.18	0.19	0.21	0.18	0.22	0.21
MgO	7.28	8.32	11.58	9.97	7.98	11.40	7.92	7.96
CaO	8.62	7.94	8.93	9.57	9.02	9.03	8.46	8.40
Na_2O	3.99	4.14	3.31	4.16	3.33	3.26	4.36	4.42
K_2O	1.70	2.20	1.81	0.76	2.07	1.88	1.63	1.64
LOI	1.99	1.57	1.42	0.51	2.00	0.87	2.36	1.63
Total	98.73	98.93	98.95	100.49	98.01	99.38	100.75	100.66
	CIPW Norm							
Q	--	--	--	--	--	--	--	--
or	10.42	13.39	10.99	4.50	12.78	11.31	9.82	9.82
ab	13.83	12.22	5.20	10.97	7.55	6.79	11.78	12.78
an	19.09	18.33	19.58	24.41	18.49	19.31	19.22	19.17
ne	11.40	12.95	12.71	13.19	11.83	11.50	14.03	13.53
wo	10.29	8.92	10.43	9.29	11.49	10.54	9.57	9.42
di en	6.68	6.42	7.93	6.78	7.58	8.01	5.93	5.93
fs	3.60	2.50	2.50	2.52	3.91	2.53	3.64	3.48
en	--	--	--	--	--	--	--	--
hy fs	--	--	--	--	--	--	--	--
fo	8.89	10.89	15.80	11.49	9.73	15.22	10.39	10.32
ol fa	5.93	5.36	6.15	7.69	6.48	6.21	7.84	7.79
mt	2.68	2.34	2.44	2.46	2.87	2.44	2.78	2.75
il	7.19	6.69	6.27	6.72	7.30	6.15	5.00	5.01
total	100.00	100.01	100.00	100.02	100.01	100.00	100.00	100.00
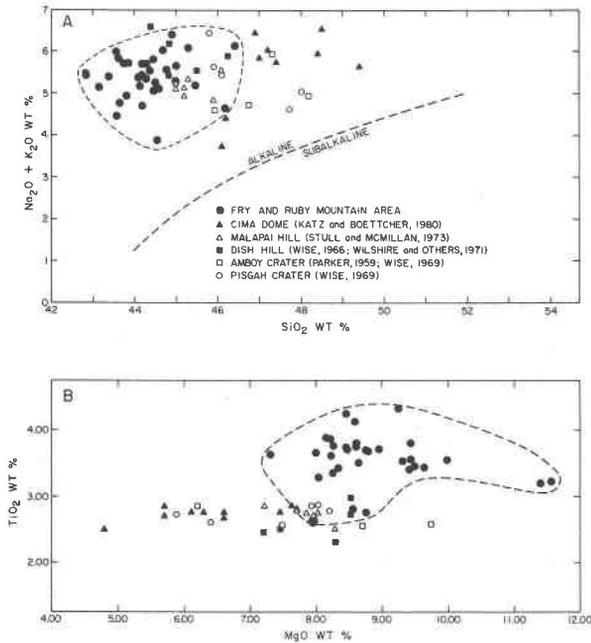
Fig. 2. Major element compositional variations of alkaline basalts from the Fry and Ruby Mountain area, in comparison to younger, Central Mojave Desert alkaline basalts. (A) Na_2O + K_2O versus SiO_2. The dashed line separates fields of alkaline and subalkaline basalts (Irvine and Barager, 1971). Dashed line encloses field for basanites from the Fry and Ruby Mountain areas. (B) TiO_2 versus MgO relationships. Symbols are the same as in (A).

in a finer-grained (<2 mm) "matrix" of recrystallized unstrained and nonrecrystallized strained grains. Olivines exhibit strain features such as undulatory extinction and kink banding; orthopyroxenes commonly exhibit undulatory extinction and bent (210) cleavage planes. The strain bands in olivine and orthopyroxene generally divide single grains into two or three zones having different optical orientations (Fig. 4d). Clinopyroxene exhibits minor strain features and spinel exhibits little.

Harzburgites possess the same mineralogic and textural features as the spinel lherzolites but contain less than 5% modal clinopyroxene. In the samples studied, brown spinel is a common accessory (0.5–2 modal %).

A single 200 gram garnet websterite inclusion (sample FMCN-2) was discovered in the Fry Mountain field. Modally this nodule consists of 36% garnet, 33% orthopyroxene, 28% clinopyroxene, 3% spinel. Orthopyroxene and clinopyroxene are anhedral to subhedral with average grain sizes of 1.0 to 1.5 mm. The orthopyroxenes have a faint brownish tint and well developed (210) cleavage. Clinopyroxenes are colorless and have poorly developed cleavage. Exsolution is rare in both pyroxenes. Garnet and spinel occur as irregular, anhedral blebs interstitial to the larger pyroxene crystals (Fig. 4a). Garnet grains have brownish rims, which in crossed polarized light appear to be composed of a radially fibrous aggregate; microprobe analysis indicates these rims are compositionally identical to the garnet. Green spinel is intimately associated with the garnet, since every spinel grain is completely or partly enclosed by an aggregate of garnet grains. A single, large (10 mm), subhedral garnet crystal was observed in one thin section

(Fig. 4a). Hand sample examination suggests such large crystals are rare. Strain features in this sample are limited to undulatory extinction and lesser bent cleavage planes within some pyroxene crystals.

A single porphyroclastic olivine websterite inclusion was found at Ruby Mountain. It contains approximately 18% forsteritic olivine, 60% enstatite, 21% diopside, and 1% brown spinel. The average grain size is 1.5 mm. Exsolution lamellae are not present in either of the two pyroxenes. Undulatory extinction is prevalent within olivine and orthopyroxene, less obvious in clinopyroxene, and not seen in spinel.

A single 400 gram amphibole-bearing inclusion (sample FMCN-1) discovered at Fry Mountain has a mode of 22% olivine, 50% clinopyroxene, 14% orthopyroxene, and 14% amphibole. Olivine (1–2 mm) is anhedral, generally ovoid, and exhibits undulatory extinction. Anhedral light green clinopyroxene (1–2 mm) is twinned and exhibits irregular, wormy exsolution of orthopyroxene. Orthopyroxene (0.75–2.5 mm) is faint pleochroic brown to colorless and has well developed (210) cleavage, anhedral to subhedral crystal form, and lamellae of exsolved clinopyroxene. Amphibole is pleochroic (dark yellow-brown to faint yellow), subhedral, and poikilitically encloses orthopyroxene, clinpyroxene, and olivine. Microprobe analyses (Table 4) indicate that this amphibole is kaersutite. Strain textures are uncommon in this sample, and although olivine and orthopyroxene display some undulatory extinction, the sample does not have a pervasive tectonite fabric. Rather, it is texturally dominated by the large poikilitic amphibole and smaller poikilitic orthopyroxene and clinopyroxene. Optically continuous amphibole poikilocrysts of dimensions 25 mm × 30 mm enclose clinopyroxene, orthopyroxene, and olivine (Fig. 4b). Recrystallized (?) orthopyroxene (non-strained, no exsolution lamellae) encloses ovoid olivine crystals as does some clinopyroxene. Several grains of partly resorbed, strained, orthopyroxene occur throughout the sample and are apparently relict crystals.

In addition to the ultramafic inclusions described above, granitoid inclusions are also commonly observed in basalts from Fry and Ruby Mountains. They were presumably derived from local Mesozoic plutons. No other types of inclusions were identified.
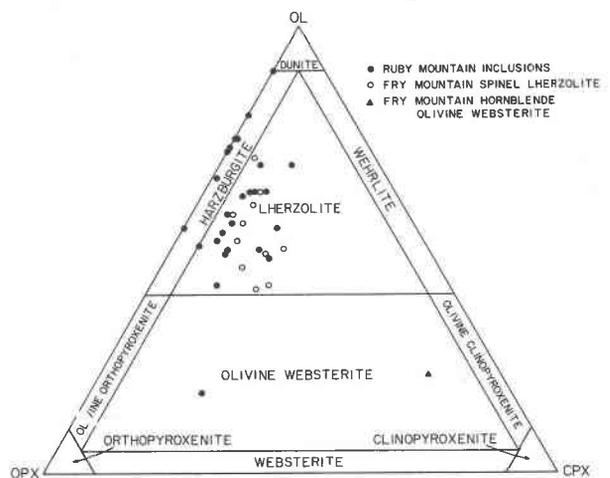

Fig. 3. Mineral modes of ultramafic inclusions from Fry and Ruby Mountains. Classification after the I.U.G.S. Subcommission on the Systematics of Igneous rocks (1973).
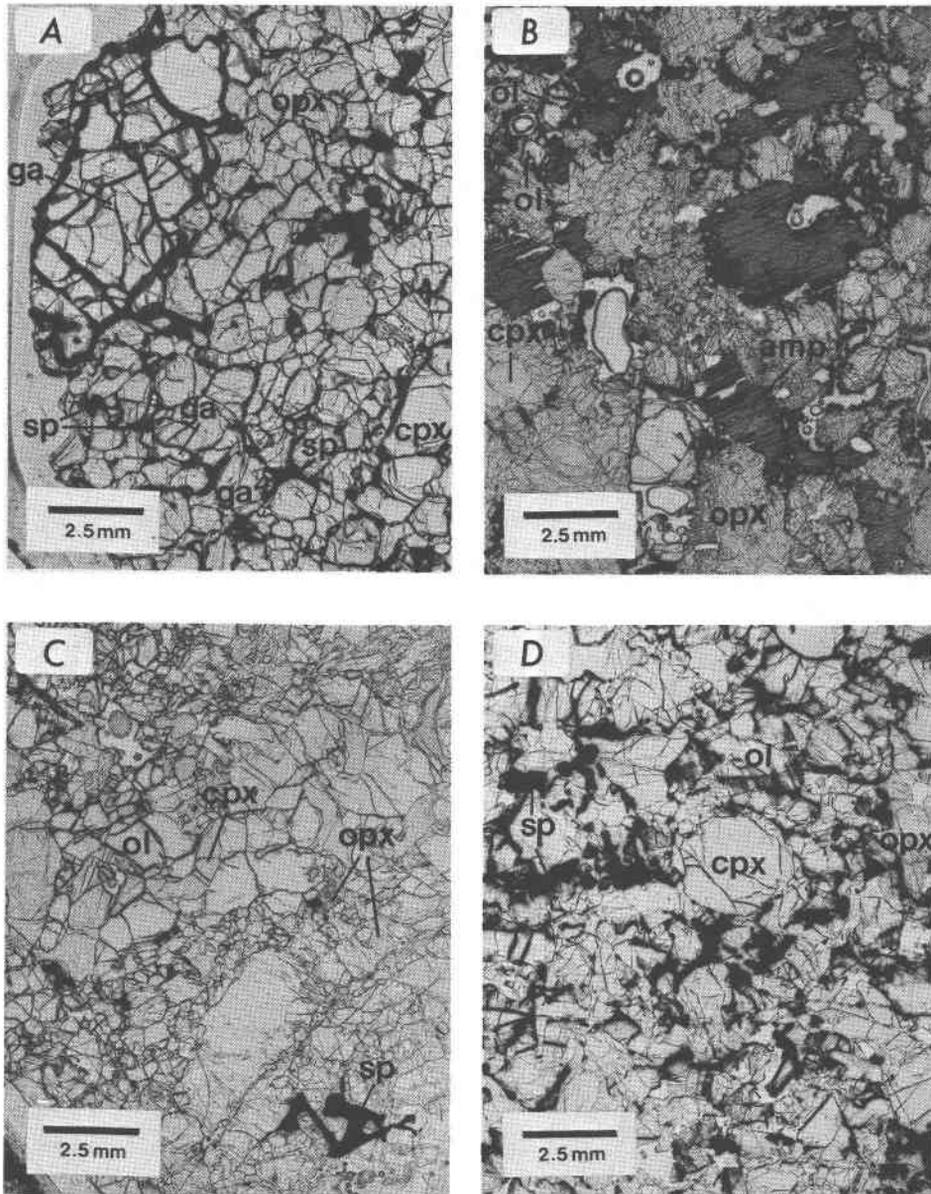
Fig. 4. Ultramafic inclusions in basanites from Fry Mountain. (A) Garnet websterite (FMCN-2) with large garnet in upper left of photograph, although most garnets form as small rims on green spinels which are interstitial to larger pyroxenes; (B) Amphibole (kaersutite) olivine websterite (FMCN-1) with large kaersutite poikilocryst enclosing olivine and pyroxenes; (C) Spinel lherzolite (FMCS-7) with typical porphyroclastic textures described in text; (D) Spinel lherzolite (FMCS-3) with strain features in olivines that have been accentuated by oxidation. Abbreviations: olivine = ol; garnet = ga; spinel = sp; clinopyroxene = cpx; orthopyroxene = opx. All photographs taken in plane-polarized light.

Inclusion mineral compositions

Minerals from six selected ultramafic inclusions were analyzed: four spinel lherzolites (i.e., samples RMA, RMD, FMCS-3, FMCS-7), the garnet websterite (FMCN-2), and the amphibole olivine websterite (FMCS-1). Analyses were performed on a MAC5 model SA3 electron microprobe operated at 15 kV and 5–50 nA sample current. Data were

reduced using real time Bence-Albee matrix corrections employing the alpha factors of Albee and Ray (1970). Representative analyses of pyroxenes, olivines, spinels, garnets, and amphiboles from these samples are presented in Tables 2–4.

Clinopyroxenes are diopsidic and exhibit little compositional variability in $Mg/(Mg + Fe)$ (Table 2 and Fig. 5). Compositions in spinel lherzolite are $En_{50-53}Wo_{41-43}$, in

Table 2. Representative compositions of pyroxenes from ultramafic inclusions and xenocrysts of Fry and Ruby Mountains

	Ruby Mountain					Fry Mountain								
	RMA	RMA	RMD	RMD	RM24B2[†]	FMCS-1	FMCS-1	FMCN-2	FMCN-2	FMCS-3	FMCS-3	FMCS-7	FMCS-7	FMB[**]
SiO_2	51.75	53.63	52.42	54.36	47.52	51.25	53.77	50.43	52.98	52.33	55.43	52.23	54.83	47.80
TiO_2	0.56	0.15	0.45	0.12	1.81	1.04	0.46	0.42	0.07	0.34	0.08	0.49	0.10	1.70
Al_2O_3	7.13	5.11	5.15	3.82	9.20	5.53	4.34	9.12	7.75	5.90	4.27	7.22	4.72	8.01
Cr_2O_3	0.71	0.38	0.78	0.38	0.00	0.59	0.10	0.32	0.19	0.95	0.44	0.70	0.26	0.01
FeO^*	3.16	6.46	2.79	9.49	8.72	5.78	11.42	3.60	7.93	2.87	6.26	2.85	6.21	10.32
MgO	14.93	31.44	15.11	30.75	12.64	15.31	29.92	14.45	31.25	15.97	33.52	15.01	32.73	11.45
CaO	18.96	0.94	20.34	0.79	17.64	19.57	1.25	21.16	0.73	20.14	0.81	19.45	0.74	19.09
Na_2O	1.95	0.14	1.90	0.22	1.74	1.28	0.09	0.53	0.02	0.98	0.05	1.36	0.07	1.70
MnO	0.14	0.13	0.08	0.18	--	0.11	0.25	0.07	0.12	0.07	0.13	0.06	0.12	---
Total	99.29	98.38	99.02	100.11	99.27	100.46	101.60	100.10	101.04	99.55	100.99	99.37	99.78	100.07

Formula Proportions Based On 4 Cations

Si	1.877	1.886	1.908	1.899	1.755	1.859	1.866	1.833	1.819	1.902	1.892	1.900	1.896	1.768
Ti	0.015	0.004	0.012	0.003	0.050	0.028	0.012	0.012	0.002	0.009	0.002	0.013	0.004	0.048
Al	0.305	0.212	0.221	0.158	0.401	0.236	0.178	0.391	0.314	0.253	0.172	0.310	0.193	0.351
Cr	0.021	0.011	0.023	0.011	--	0.017	0.003	0.009	0.005	0.027	0.012	0.020	0.007	---
Fe	0.096	0.190	0.085	0.277	0.269	0.176	0.332	0.110	0.228	0.087	0.179	0.087	0.180	0.321
Mg	0.807	1.649	0.820	1.602	0.696	0.828	1.548	0.783	1.600	0.865	1.706	0.814	1.687	0.621
Ca	0.737	0.035	0.794	0.030	0.698	0.761	0.047	0.824	0.027	0.785	0.030	0.758	0.027	0.777
Na	0.137	0.009	0.135	0.015	0.125	0.090	0.007	0.037	0.001	0.070	0.004	0.096	0.005	0.123
Mn	0.004	0.004	0.002	0.005	--	0.003	0.008	0.002	0.004	0.002	0.004	0.002	0.004	---

*: All Fe calculated as FeO.
†: Ruby Mountain clinopyroxene megacryst.
**: Fry Mountain clinopyroxene megacryst.

the amphibole olivine websterite (FMCS-1) are close to $En_{49}Wo_{40}$, and in the garnet websterite average $En_{50}Wo_{42}$. Al_2O_3 contents for diopsides range from 5.2 to 7.4 wt.% in lherzolites, average 5.5 wt.% in amphibole olivine websterite, and are 9.1 wt.% in garnet websterite.

Orthopyroxenes are Mg-rich with compositions En_{85-90} (Table 2 and Fig. 5). Mg–Fe partitioning between enstatite and coexisting olivine is essentially 1:1 for both peridotite inclusions and amphibole olivine websterite and is 1:1 between orthopyroxene and clinopyroxene except for spinel lherzolite inclusion RMD. Alumina contents of enstatites in periododite inclusions range from 3.1 to 5.8 wt.% and in garnet websterite alumina averages 7.8 wt.%. Although clinopyroxene exsolution was observed in several samples,

it could not be analyzed due to the small width of lamellae. Al_2O_3 contents of coexisting spinel and either enstatite or diopside exhibit a positive linear relationship as noted by Carswell (1980) and Brown et al. (1980). Clinopyroxene megacrysts are either titaniferous augites or titaniferous salites ($En_{38-42}Wo_{36-42}$, Fig. 5). All clinopyroxene megacrysts are higher in Al, Ti, and total Fe and lower in Mg, Cr, and Ca than clinopyroxenes from spinel lherzolite. Charge balance considerations require that virtually all iron in pyroxenes from both inclusions and megacrysts be divalent.

Olivines (Table 3) from 3 of the 4 lherzolite nodules have a restricted Mg/(Mg + Fe) compositional range between $Fo_{89.3}$ and $Fo_{90.3}$. Inclusions RMD and FMCS-1 (amphibole olivine websterite) contain olivines whose compositions are close to Fo_{82}. Both RMD and FMCS-1 exhibit textures (e.g., RMD pyroxenes exhibit spongy border zones and FMCS-1 contains poikilitic amphibole) which imply partial re-equilibration at $P–T$ conditions different than the conditions of initial formation.

Spinels exhibit significant compositional variability in Cr and Al (Table 3). In lherzolites, Cr_2O_3 ranges from 8.4 to 19.2 wt.% and Al_2O_3 from 45.5 to 59.9 wt.%. Spinels in garnet websterite average 3.5 wt.% Cr_2O_3 and 64.1 wt.% Al_2O_3. Mg and Fe content varies also, but not as much as Cr and Al. Trace amounts of Mn occur in the tetrahedral sites of most spinels. The compositions of spinels in terms of Cr × 100/(Cr + Al) and Mg × 100/(Mg + Fe²⁺) are illustrated in Figure 6. Irvine (1967) has defined a field for spinels from ultramafic nodules in alkaline volcanics and
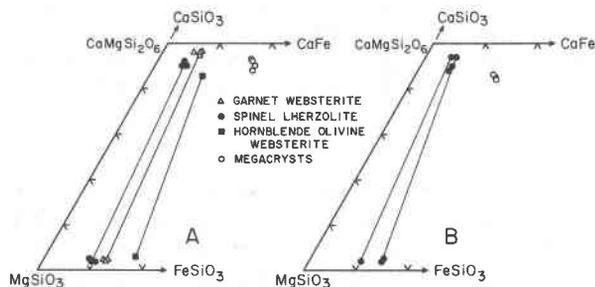

Fig. 5. Quadrilateral compositions of pyroxenes from inclusions and megacrysts from Fry (A) and Ruby (B) Mountains. Tie lines connect compositions of coexisting orthopyroxene and clinopyroxene used in geothermometric calculations.

Table 3. Representative compositions of olivines and spinels from Fry and Ruby Mountain inclusions

| | Olivines | | | | | Spinels | | | | |
	RMA	RMD	FMCS-1	FMCS-3	FMCS-7	RMA	RMD	FMCM-2	FMCS-3	FMCS-7
SiO_2	40.46	39.50	39.13	40.93	40.99	0.13	0.17	0.13	0.14	0.18
TiO_2	0.01	0.01	0.03	0.00	0.00	0.14	0.09	0.03	0.12	0.11
Al_2O_3	0.00	0.00	0.00	0.00	0.00	58.02	46.20	63.94	53.15	59.92
Cr_2O_3	0.00	0.00	0.03	0.04	0.00	9.18	19.65	3.52	13.35	8.45
FeO^1	10.15	16.85	15.92	9.39	9.89	10.63	17.84	11.69	14.25	11.24
MgO	48.28	43.43	43.12	50.56	50.36	19.89	15.29	20.09	20.45	21.26
CaO	0.07	0.07	0.09	0.08	0.07	0.00	0.00	0.00	0.00	0.00
MnO	0.18	0.29	0.23	0.15	0.13	0.11	0.28	0.05	0.02	0.11
NiO	0.45	0.37	0.23	0.43	0.42	--	--	--	--	--
Total	99.60	100.52	98.78	101.58	101.86	98.10	99.52	99.45	101.48	101.27

Formula Proportions Based On 3 Cations

Si	0.9988	0.9961	1.0011	0.9843	0.9846	0.0033	0.0047	0.0032	0.0036	0.0044
Ti	0.0001	0.0002	--	--	--	0.0027	0.0018	0.0005	0.0023	0.0021
Al	--	--	--	--	--	1.7915	1.5084	1.9136	1.6213	1.7831
Cr	--	--	0.0006	0.0007	--	0.1901	0.4304	0.0707	0.2731	0.1686
Fe	0.2095	0.3554	0.3407	0.1890	0.1988	0.2329	0.4132	0.2483	0.3085	0.2373
Mg	1.7771	1.6328	1.6448	1.8126	1.8037	0.7768	0.6314	0.7606	0.7887	0.8004
Ca	0.0017	0.0019	0.0024	0.0020	0.0020	--	--	--	--	--
Mn	0.0038	0.0061	0.0050	0.0030	0.0026	0.0024	0.0064	0.0010	0.0005	0.0022
Ni	0.0088	0.0074	0.0048	0.0082	0.0082	--	--	--	--	--
Fo	89.3	81.8	82.6	90.4	89.9					

1: Total Fe calculated as FeO.

kimberlites, and most spinels plot within this field. The only exceptions are in one lherzolite nodule (FMCS-7) and the garnet webseterite (FMCN-2). The spinels are compositionally similar to those in peridotite at Cima Dome and Dish Hill and to spinel in the Dish Hill garnet clinopyroxenite (Fig. 6).

Garnets in the garnet websterite (FMCN-2) are $Py_{68}Al_{18}Gr_{12}$ (Table 4). The garnets exhibit negligible zoning or differences in composition whether they occur as discrete grains or as rims on spinel. The garnets from this inclusion are compositionally similar to those in the Dish Hill garnet clinopyroxenite (i.e., $Py_{63}Al_{23}Gr_{14}$, Shervais and others, 1973) except that the Fry Mountain garnets contain 1 wt.% less Al_2O_3 and about 1 wt.% more MgO.

Kaersutite poikilocrysts comprise approximately 14% of the mineral mode of inclusion FMCS-1 from Fry Mountain. Cognate megacrysts of kaersutite from Ruby Mountain (Table 4) have lower MgO and Na_2O, slightly lower Cr_2O_3, and higher K_2O and total iron. The Dish Hill vein amphibole in peridotite (Wilshire and others, 1971) is almost identical in major element composition to the amphibole in sample FMCS-1.

Thermobarometry

The pressure–temperature crystallization conditions of ultramafic inclusions can be estimated or at least bracketed by assuming equilibrium partitioning of cations among coexisting minerals. Numerous reliable geothermometers are available, although geobarometers (particularly for spinel lherzolites) are limited. Since compositional zoning within minerals from individual inclusions from Ruby and

Fry Mountains is minimal, the compositions presented in Tables 2–4 were used in all calculations.

The most commonly used geothermometers are based on Fe/Mg partitioning between coexisting clinopyroxene and
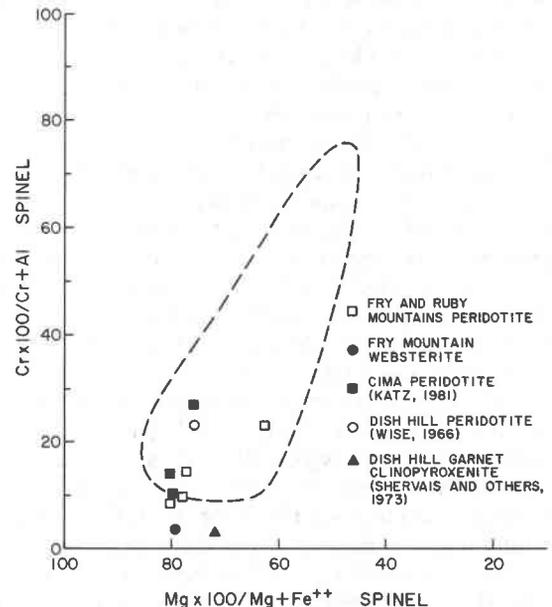

Fig. 6. Cr/(Cr + Al) versus Mg/(Mg + Fe^{++}) compositional relationships of spinels in ultramafic inclusions from Fry and Ruby Mountains and other Mojave Desert localities. Dashed line encloses the approximate field of spinels in peridotite inclusions and kimberlites as defined by Irvine (1967).

Table 4. Representative compositions of garnet and amphibole from Fry Mountain websterite inclusions and amphibole megacrysts from Ruby Mountain

| | Garnet | Amphibole | |
	FMCN-2	FMCS-1	RM2DB[1]
SiO_2	42.56	40.69	39.88
TiO_2	0.13	4.96	5.04
Al_2O_3	23.98	13.61	13.44
Cr_2O_3	0.47	0.17	0.23
$FeO[2]$	9.23	8.30	13.86
MgO	19.35	15.05	10.70
CaO	5.35	10.80	10.43
MnO	0.31	.10	.14
K_2O	—	1.32	1.85
Na_2O	—	3.02	2.77
Total	101.38	98.04	98.34
	8 Cations	15 Cations (Minus Na,K)	
Si	2.9898	6.0045	6.0695
Ti	.0066	.5511	.5777
Al	1.9868	2.3678	2.4126
Cr	.0261	.0194	.0279
Fe	.5423	1.0250	1.7649
Mg	2.0275	3.3118	2.4290
Ca	.4025	1.7074	1.7005
Mn	.0184	.0129	.0177
K	—	.2482	.3595
Na	—	.8701	.8191

1: megacryst
2: Total Fe as FeO

orthopyroxene. Table 5 presents the result of calculations based on the methods of Mori (1977), Wells (1977), and Wood and Banno (1973) for six Fry and Ruby Mountain ultramafic inclusions. Calculated temperatures for individual inclusions generally have a 200°C scatter; the Mori geothermometer yields the highest estimates and the Wells method the lowest. The temperatures range from a minimum 934°C (Wells geothermometer on RMD) to a maximum of 1255°C (Mori geothermometer on FMCS-1). For any one particular method, however, temperatures calculated for the entire suite do not vary by more than 75°C. All of the calculated temperatures are similar to or lower than the 1200–1300°C liquidus temperatures estimated for basanitic melts at pressures between 25 and 30 kbar, with H_2O contents between 2 and 7 wt.% (Green, 1973). Thus all the inclusions probably equilibrated at comparable temperatures, not far removed from those of the source regions of their basanitic melt hosts.

Geobarometric estimates for ultramafic inclusions are predominantly based on Al_2O_3 solubility in orthopyroxenes (e.g., MacGregor, 1974). Unfortunately, the alumina isopleths within the spinel field are not particularly pressure sensitive (see Hertzberg, 1978, Fig. 6). Minimum pressures for Ruby and Fry Mountain inclusions, calculated using Hertzberg's (1978) equation 31, are approximately 36 kbar, which is unreasonably high for spinel lherzolites.

Recently, a geobarometer based on calcium content of olivine coexisting with orthopyroxene and clinopyroxene was suggested by Finnerty and Rigden (1981). They demonstrated a method that produces petrologically reasonable results when temperatures are calculated using the method of Wells (1977). Olivines in ultramafic inclusions from Fry and Ruby Mountain range from 0.06 to 0.13 wt.% CaO, thus yielding a pressure range of 19–28 kbar by assuming a mean CaO content of 0.08 and a possible temperature range of 930–1000°C.

Maximum pressures of stability for spinel lherzolite in the CMAS system have been experimentally delineated by a number of workers (e.g. MacGregor, 1965; O'Hara et al., 1971; Newton, 1978; and O'Neill, 1981). Recently, O'Neill (1981) has experimentally investigated the effects of Cr_2O_3 on the spinel–garnet transition. At a given isotherm, increasing Cr_2O_3-content of spinel will dramatically increase the equilibrium pressure for the reaction: spinel + orthopyroxene = garnet + olivine. Assuming 1000°C for the equilibrium temperature of the Fry and Ruby Mountain inclusions, the range in Cr_2O_3 content of spinels (3.5 to 19.7 wt.% Cr_2O_3, Table 3) yields equilibrium pressures of 18–23 kbar. If FeO contents of inclusion olivines (which average Fo_{90}) are accounted for, these pressures are lowered to approximately 15–20 kbar (O'Neill, 1981, Fig. 5).

The Fry Mountain garnet websterite must also have equilibrated at pressures below 20–23 kbar if the observed assemblage of orthopyroxene, clinopyroxene, spinel, and garnet is stable. The spinel–garnet transition in peridotites is defined by the reaction: spinel + orthopyroxene = garnet + olivine (O'Neill, 1981). Thus in the model system, $MgO–SiO_2–Al_2O_3$, the three phase sub-assemblage of orthopyroxene + garnet + spinel is stable on the lower pressure (and/or higher temperature) side of this reaction, for bulk compositions (such as websterites) that are MgO-depleted with respect to lherzolites or harzburgites. Reconnaissance calculations based on a combination of estimated modes and mineral compositions indicate that the garnet websterite (FMCN-2) inclusion has significantly lower $(MgO/(MgO + Al_2O_3 + SiO_2)(=0.26)$ than does a representative spinel lherzolite inclusion (e.g., FMCS-3 with mode of 46% olivine, 38% orthopyroxene, 13% clinopyroxene, and 3% spinel, and $MgO/(MgO + Al_2O_3 + SiO_2) = 0.43$) from the same locality. The temperature estimates (Table 5) do not indicate that the garnet websterite inclusion equilibrated at significantly different conditions than the spinel lherzolites from Fry Mountain. Therefore, we suggest that the garnet websterite inclusion

Table 5. Equilibration temperatures for ultramafic inclusions from Fry and Ruby Mountains, based on various two pyroxene geothermometers

	Mori (1977)	Wells (1977)	Wood & Banno (1973)
RMD	1188 ± 35	934 ± 70	1009 ± 60
RMA	1178 ± 35	952 ± 70	1053 ± 60
FMCS-7	1220 ± 35	984 ± 70	1085 ± 60
FMCS-3	1233 ± 35	1003 ± 70	1102 ± 60
FMCS-1	1255 ± 35	992 ± 70	1037 ± 60
FMCN-2	1197 ±35	955 ± 70	1041 ± 60

most likely derived by recrystallization of a more aluminous, less MgO-rich protolith than did the spinel lherzolites, but apparently under similar conditions, temperatures between 950 and 1200°C and pressures below 23 kbar. Further evidence for a relatively low pressure origin of the garnet websterite inclusion is indicated by garnet-orthopyroxene barometry (equation 5 of Harley and Green, 1982), which yields equilibrium pressures of approximately 10 kbar.

All of the ultramafic inclusions found at Fry and Ruby Mountains are interpreted to be accidental upper mantle fragments as indicated by their tectonite textures, mineral assemblages, and thermobarometry. The kaersutite-bearing olivine websterite inclusion is also interpreted to be an accidental upper mantle fragment that has been subjected to mantle metasomatism (e.g., Wilshire et al., 1980; Boettcher and O'Neil, 1980). The depth to the mantle in the Mojave and adjacent San Bernardino Mountains is estimated to be between 30 and 35 km (Hadley and Kanamori, 1977). Thus, minimum pressures for mantle-derived inclusions are between 8.5 and 10.0 kbar, consistent with the barometric calculations and the plagioclase–spinel transition (Green and Hiberson, 1970).

Garnet websterite

Garnet-bearing peridotite has been classified as a distinct nodule group, the garnetiferous ultramafic group, by Wilshire and Shervais (1975); according to them this inclusion type does not belong to the Cr-spinel series. Garnet peridotite is extremely rare in basaltic rocks and when present is thought to represent accidental upper mantle fragments (Shervais et al., 1973). It is believed that the garnet websterite collected at Fry Mountain is only the second garnet-bearing inclusion in basalt to be found in the western United States, the first being a garnet clinopyroxenite discovered at Dish Hill (Shervais et al., 1973). Other garnet peridotite discoveries in the western United States have been confined to kimberlite hosts in the Colorado Plateau region (e.g., Helmstaedt and Doig, 1975).

The garnet websterite of Fry Mountain and the garnet clinopyroxenite of Dish Hill have dissimilar modal compositions (Fig. 3). Orthopyroxene, garnet, and spinel are enriched in the Fry Mountain inclusion relative to the Dish Hill inclusion. Mineral compositions, however, do not differ significantly.

Texturally, these two inclusions share some common features: (1) both exhibit tectonic deformation textures; (2) garnet occurs mainly as reaction rims on spinel and as subordinate distinct grains; and (3) recrystallization textures are present. Important textural dissimilarities are: (1) grain sizes differ greatly between the two and (2) exsolution features are prevalent throughout the Dish Hill sample and are rare in the Fry Mountain inclusion.

To explain its deformation and recrystallization textures Shervais et al. (1973) interpreted the Dish Hill garnet clinopyroxenite as an accidental inclusion derived from the upper mantle. They believe that garnet formed in the Dish Hill sample by subsolidus reaction between clinopyroxene and spinel and by exsolution from clinopyroxene. The garnet websterite from Fry Mountain is also an accidental upper mantle fragment, but lacks textural indications of recrystallization by the reaction mechanisms postulated for Dish Hill.

Alkaline basaltic volcanism of the Mojave Desert region

The outcrop characteristics, bulk chemical composition, and mineralogy of the basalt province that includes the Fry and Ruby Mountain localities resemble those of the other late Cenozoic, alkaline basalts farther north in the Mojave Desert. The entire set of Mojave occurrences is in turn correlative (Glazner, 1981; Katz and Boettcher, 1980), with the late Cenozoic alkaline volcanism of the Basin and Range province (Leeman and Rogers, 1970; Best and Brimhall, 1974)—a tectonic setting characterized by high heat flow and a thinning crust. In both the Basin Range and Mojave Desert provinces, magmas appear to have been generated at depths ranging from 40 to 60 km by no more than 20% partial melting of a peridotite mantle (Leeman and Rogers, 1970).

The MgO–SiO$_2$–TiO$_2$ contents, the tectonic setting and the detailed age distributions do, however, reveal significant differences between the basalts that bear inclusions at the Fry and Ruby Mountain localities and their counterparts to the north in the Central Mojave. The Fry and Ruby Mountain basalts are relatively primitive (i.e., somewhat richer in MgO) and this may reflect changes in the pressures, temperatures, or compositions of source regions for the alkaline basaltic magmas during the last 10 m.y. Available age determinations indicate that the alkaline basaltic volcanism in the Fry and Ruby Mountain area began no more than 10 m.y. ago and ceased approximately 6 m.y. ago. The latest age assessments for alkaline basalts in the Central Mojave (Dohrenwend et al., 1984) indicate that the volcanism began approximately 6 m.y. ago and has continued into historic time.

The Fry and Ruby Mountain localities are part of a basalt province that is preserved in the eastern San Bernardino Mountains and immediately adjacent basins. This part of the Transverse Ranges belonged to the Mojave Block until the onset of a late Cenozoic, transpressional uplift (Sadler, 1982) that was probably a response to the local orientation of the San Andreas fault. Although the most spectacular uplift, associated with thrust faults, appears to have occurred 2–3 m.y. ago, Sadler and Reeder (1983) argue that the 4–6 m.y. inception of basin formation at the sites of later thrust faulting is the first record of transpressional tectonics. One experimental model of transpressional uplift (Bartlett et al., 1981) indicates a mushroom-like cross section with a deep, tapered "root" zone. The local termination of alkaline basalt volcanism in and near the San Bernardino Mountains and its northward shift coincident with the onset of transpressional effects

may be evidence of "root" zone influences as deep as 40–60 km—the likely depth of magma genesis.

Acknowledgments

References

Albee, A. L. and Ray, L. (1970) Correction factors for electron probe microanalysis of silicates, oxides, carbonates, phospates, and sulfides. Analytical Chemistry, 42, 1409–1414.

Bartlett, W. L., Friedman, M., and Logan, J. M., 1981, Experimental folding and faulting of rocks under confining pressure. Part IX, wrench faults in limestone layers. Tectonophysics, 79, 255–277.

Best, M. G. and Brimhall, W. H. (1974) Late Cenozoic alkalic basaltic magmas in the western Colorado plateau and the Basin and Range transition zone, U.S.A. and their bearing on mantle dynamics. Geological Society of America Bulletin, 85, 1677–1690.

Boettcher, A. L. and O'Neil, J. R. (1980) Stable isotope, chemical, and petrographic studies of high-pressure amphiboles and micas: evidence for metasomatism in the mantle source regions of alkali basalts and kimberlites. American Journal of Science, 280-A, 594–621.

Brown, G. M., Pinsent, R. H., and Cisy, P. (1980) The petrology of spinel-peridotite xenoliths from the Massif Central, France. American Journal of Science, 280-A, 471–498.

Carswell, D. (1980) Mantle derived lherzolite nodules associated with kimberlite, carbonatite, and basalt magmatism: A review. Lithos, 13, 121–138.

Dohrenwend, J. C., McFadden, L. D., Turrin, B. D., and Wells, S. G. (1984) K–A dating of the Cima volcanic field, eastern Mojave Desert, California: Late Cenozoic volcanic history and landscape evolution. Geology, 12, 163–167.

Finnerty, A. A. and Rigden, S. M. (1981) Olivine barometry: application to pressure estimation for terrestrial and lunar rocks. (Abstr.) 12th Lunar Science Conference, part 1, 279–281.

Glazner, A. (1981) Cenozoic evolution of the Mojave Block and adjacent areas. Ph.D. dissertation, University of California, Los Angeles.

Green, D. H. (1973) Conditions of melting of basanite magma from garnet peridotite. Earth and Planetary Science Letters, 17, 456–465.

Green, D. H. and Hibberson, W. (1970) The instability of plagioclase in peridotite at high pressures. Lithos, 3, 209–221.

Hadley, D. and Kanomori, H. (1977) Seismic structure of the Transverse Ranges, California. Geological Society of America Bulletin, 88, 1469–1478.

Harley, S. L. and Green, D. H. (1982) Garnet–orthopyroxene barometry for granulites and peridotites. Nature, 300, 697–701.

Helmstaedt, H. and Doig, R. (1975) Eclogite nodules from kimberlite pipes of the Colorado Plateau—sample of subducted Franciscan-type oceanic lithosphere. Physics and Chemistry of the Earth, 9, 95–111.

Hertzberg, C. (1978) Pyroxene geothermometry and geobarometry: experimental and thermodynamic evaluation of some subsolidus phase relations involving pyroxenes in the system CaO–MgO–Al₂O₃–SiO₂. Geochimica et Cosmochimica Acta 42, 945–957.

Irvine, T. N. (1967) Chromian spinel as a petrologic indicator, part 2: petrologic applications. Canadian Journal of Earth Science, 4, 71–103.

Irvine, T. N. and Baragar, W. R. A. (1971) A guide to chemical classification of the common volcanic rocks. Canadian Journal of Earth Science, 8, 523–548.

I.U.G.S. Subcommission on the Systematics of Igneous Rocks (1973) Classification and nomenclature of plutonic rocks: recommendations. Neues Jahrbuch für Mineralogie Monatsheft, 4, 149–164.

Katz, M. M. (1981) Geology and geochemistry of the southern part of the Cima volcanic field: Unpublished M.S. thesis, Univ. of California, Los Angeles.

Katz, M. M. and Boettcher, A. (1980) The Cima volcanic field. In D. L. Fife and A. R. Brown, Eds., Geology and Mineral Wealth of the California Desert, p. 236–241. South Coast Geological Society.

Leeman, W. P. and Rogers, J. J. W. (1970) Late Cenozoic alkaliolivine basalts of the Basin-Range province, U.S.A. Contributions to Mineralogy and Petrology, 25, 1–24.

MacGregor, I. D. (1965) Stability fields of spinel and garnet peridotites in the synthetic system MgO–CaO–Al₂O₃–SiO₂. Carnegie Institute Washington Yearbook, 64, 126–134.

MacGregor, I. D. (1974) The system MgO–Al₂O₃–SiO₂: solubility of Al₂O₃ in enstatite for spinel and garnet peridotite compositions. American Mineralogist, 59, 110–119.

Mori, T. (1977) Geothermometry of spinel lherzolites. Contributions to Mineralogy and Petrology, 59, 261–279.

Neville, S. L. (1982) Late Miocene alkaline volcanism, southcentral Mojave Desert and northeast San Bernadino Mountains, California, unpublished M.S. thesis, U. C. Riverside.

Neville, S. L. and Chambers, J. M. (1982) Late Miocene alkaline volcanism, northeastern San Bernardino mountain and adjacent Mojave Desert. In J. D. Cooper, compiler, Geologic Excursions in the Transverse Ranges, Southern California, Geological Society of America 78th Annual Meeting Guidebook, Cordilleran Section, 103–106.

Newton, R. C. (1978) Experimental determination of the spinel peridotite to garnet peridotite reaction in the system MgO–Al₂O₃–SiO₂ in the range 900–1100°C and Al₂O₃ isopleths of enstatite in the spinel field. Contributions to Mineralogy and Petrology, 66, 189–201.

Oberlander, T. M. (1972) Morphogenesis of granitic boulder slopes in the Mojave Desert, California. Journal of Geology, 80, 1–19.

O'Hara, M. H., Richardson, S. W., and Wilson, G. (1971) Garnet peridotite stability and occurrence in crust and mantle. Contributions to Mineralogy and Petrology, 32, 48–68.

O'Neill, H. C. (1981) The transition between spinel lherzolite and garnet lherzolite, and its use as a geobarometer. Contributions to Mineralogy and Petrology, 77, 185–194.

Pike, J. E. N. and Schwarzman, E. C. (1977) Classification of textures in ultramafic xenoliths. Journal of Geology, 85, 49–61.

Parker, R. B. (1959) Magmatic differentiation of Amboy Crater, California. American Mineralogist, 44, 656–658.

Peterson, D. (1976) Patterns of Quaternary denundation and deposition at Pipes Wash, Mojave Desert, California Ph.D. dissertation, University of California, Riverside.

Sadler, P. M. (1982) Provenance and structure of late Cenozoic sediments in the northeast San Bernadino Mountains. In J. D. Cooper, compiler, Geologic Excursions in the Transverse Ranges, Southern California: Geological Society of America. 78th Annual meeting. Guidebook, Cordilleran Section, 83–91.

Sadler, P. M. and Reeder, W. A. (1983) Upper Cenozoic, quartzite-bearing gravels of the San Bernardino Mountains, Southern California: recycling and mixing as a result of transpressional uplift. In D. W. Andersen and M. J. Rymer, Eds., Tectonics and Sedimentation along Faults of the San Andreas System, p. 45–57. Pacific Section, Society of Economic Mineralogists and Paleontologists, Los Angeles.

Shervais, J. W., Wilshire, H. G., and Schwarzman, E. C. (1973) Garnet clinopyroxenite xenolith from Dish Hill, California. Earth and Planetary Science Letters, 19, 120–130.

Stull, R. J. and McMillan, K. (1973) Origin of lherzolite inclusions in the Malapai Hill basalt, Joshua Tree National Monument, California. Geological Society of America Bulletin, 84, 2343–2350.

Wells, P. R. A. (1977) Pyroxene thermometry in simple and complex systems. Contributions to Mineralogy and Petrology, 62, 129–139.

Wilshire, H. G., Pike, J. E. N., Meyer, C. E., and Schwarzman, E. C. (1980). Amphibole-rich veins in lherzolite xenoliths, Dish Hill and Deadman Lake, California. American Journal of Science, 280-A, 576–593.

Wilshire, H. G. and Shervais, J. W. (1975) Al-augite and Cr-diopside ultramafic xenoliths in basaltic rocks from the western United States. In L. H. Ahrens et al., Eds., Physics and Chemistry of the Earth, 9, p. 257–272. Pergamon, New York.

Wilshire, H. G. and Trask, N. J. (1971) Structural and textural relationships of amphibole and phlogopite in peridotite inclusions, Dish Hill, California. American Mineralogist, 56, 255.

Wilshire, H. G., Calk, L. C., and Schwarzman, E. C. (1971) Kaersutite—a product of reaction between paragasite and basanite at Dish Hill, California. Earth Science Letters, 10, 281–284.

Wise, W. S. (1966) Zeolitic basanite from southeastern California Bulletin of Volcanology, 29, 235–252.

Wise, W. S. (1969) Origin of basaltic magmas in the Mojave Desert area, California. Contributions to Mineralogy and Petrology, 23, 53–64.

Wood, R. J. and Banno, S. (1973) Garnet–orthopyroxene and orthopyroxene–clinopyroxene relationships in simple and complex systems. Contributions to Mineralogy and Petrology, 42, 109–124.